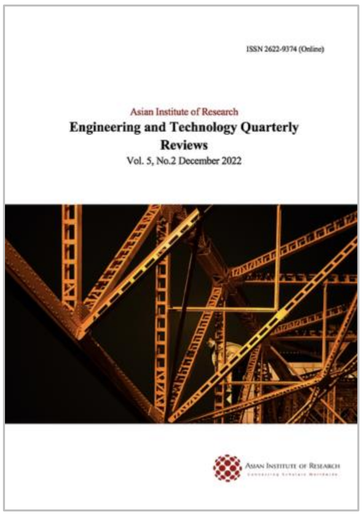

Engineering and Technology Quarterly Reviews

Eski, Ö, & Enbia, H. A. I. (2023), The Effect of Rolling Temperature and Rolling Ratio on Hardness and TRS of 90μm Grain Size on B_4C %5 Reinforcement Copper Matrix Composite. In: *Engineering and Technology Quarterly Reviews*, Vol.6, No.1, 9-20.

ISSN 2622-9374

The online version of this article can be found at:
https://www.asianinstituteofresearch.org/

Published by:
The Asian Institute of Research

The Asian Institute of Research *Engineering and Technology Quarterly Reviews* is a peer-reviewed International Journal. The journal covers scholarly articles in the fields of Engineering and Technology, including (but not limited to) Civil Engineering, Informatics Engineering, Environmental Engineering, Mechanical Engineering, Industrial Engineering, Marine Engineering, Electrical Engineering, Architectural Engineering, Geological Engineering, Mining Engineering, Bioelectronics, Robotics and Automation, Software Engineering, and Technology. As the journal is Open Access, it ensures high visibility and the increase of citations for all research articles published. The *Engineering and Technology Quarterly Reviews* aims to facilitate scholarly work on recent theoretical and practical aspects of Education.

Asian Institute of Research
Connecting Scholars Worldwide

The Asian Institute of Research
Engineering and Technology Quarterly Reviews
Vol.6, No.1, 2023: 9-20
ISSN 2622-9374

The Effect of Rolling Temperature and Rolling Ratio on Hardness and TRS of 90µm Grain Size on B_4C %5 Reinforcement Copper Matrix Composite

Özkan Eski[1], Hasan AlSead Ibrahim Enbia[2]

[1,2] Kastamonu University, Engineering Faculty, Department of Metallurgy and Materials Engineering Kuzeykent Campus, Kastamonu, Turkey ozkaneski@kastamonu.edu.tr, Enbayahasan@gmail.com

Abstract
This study investigates how adding boron carbide (B_4C) 5%wt. with a grain size of 90µm, affected the mechanical and physical characteristics of cold-pressed copper boron carbide (Cu-B_4C) compounds, including their fine structure, hardness, and density. Commercial Cu powders with a particle size of 40 µm were modified by adding 5% by weight of B_4C, which has a particle size of 90µm. For 120 minutes, the Cu-B_4C compounds were sintered in argon at 850°C. The values obtained before and after hot rolling were compared. Some samples were hot-rolled at rolling temperatures of 600°C, 700°C, 800°C with rolling pressures of (10%,20%,30%,40%). Sintered materials before and after hot rolling were examined, using SEM-EDS, to compare density, hardness, and bending resistance. It was discovered that B_4C was evenly distributed throughout the Cu matrix in the SEM-EDS images that were obtained. As the B_4C ratio increased, the density of the original materials reduced, and their porosity increased, the hardness of the composites also increased. With an increase in the rolling ratio and the rolling pressure ratios by (10%,20%,30%, 40%), the values of hardness and flexural strength of the rolled samples fell, and the hardness decreased at 800°C for all the samples that were exposed to these factors (Saravanapandi Solairajan.Aa et al., 2007) (Chandra et al., 2015).

Keywords: Metal Matrix Composites, Cu, B_4C, Cold Pressing, Hot Rolling

1. Introduction

A composite material is made by combining two or more materials, often ones that have very different properties. The two materials work together to give the composite its unique properties. The reinforcing component is typically distributed as a continuous or matrix component. When the matrix is a metal, the composite is termed a metal-matrix composite (MMC). In MMCs, the reinforcement usually takes the form of particles, whiskers, short fibers, or continuous fibers (Saravanapandi Solairajan.Aa* et al., 2007). Composite materials have been utilized to solve technological problems for a long time, but only in the 1960s did these materials start capturing the attention of industries with the introduction of polymeric based, metal matrix based composites. In composite materials, the reinforcements can be fibers, particulates, or whiskers, and the matrix materials can be metals, plastics, or ceramics. The reinforcements can be made from polymers, ceramics, or metals(Chandra et al., 2015). In recent years, the development of materials has changed from monolithic to composite materials to meet the global need for structural materials with decreased weight, low cost, high quality, and performance. Performance, financial, and environmental advantages are the driving forces behind MMCs use in the aerospace and automotive industries. Metal-matrix composites (MMCs), which have been rising in popularity, have been trending in the opposite direction. MMCs have advantages over base metal alloys due to the incorporation of a non-metallic reinforcement within a metallic matrix. Improvements in thermal conductivity, resistance to abrasion and wear, creep resistance, dimensional stability, and extraordinarily high stiffness-to-weight and strength-to-weight ratios are a few of these. They function better at high temperatures as well. The thermo-mechanical characteristics and performance of the light weight but relatively soft host metal are enhanced by the addition of hard and strong particulates or fibers. Ceramics like silicon carbide and alumina, B4C, AlN, TiC, TiB2, TiO2, and hard metals like titanium and tungsten are examples of common reinforcement materials (Sahu & Banchhor, 2016).

Copper (Cu) is one of the most versatile engineering materials available. The combination of physical properties such as strength, conductivity, corrosion resistance, machinability, and ductility makes copper suitable for a wide range of applications. One of the most extensively used structural and functional metals for several engineering applications thanks to its excellent electrical and thermal conductivity, copper is an indispensable metal in the electrical and electronics industries because it has good ductility and is highly resistant to corrosion and oxidation. The properties that drive the use of copper include, in addition to, high electrical and thermal conductivities, favorable combinations of strength and ductility, ease of fabrication (machinability, castability, weldability, and joining properties), aesthetic appeal, and the metal’s ability to form literally hundreds of useful alloys, usually with specifically tailored properties (Konen & Fintov, 2012). Boron carbide (B_4C) is a non-oxide ceramic that comes in the same category as non-metallic hard materials such as silicon carbide, cubic boron nitride, and diamond. Boron-carbon materials were first produced by Joly in 1883, then by Moissan in 1894. However, it was not until 1934 that Ridgway analyzed the composition of such boron-carbon compounds and designated B_4C as the chemical formula for stoichiometric (B_4C). Boron carbide (B_4C) is characterized by its high hardness (2950 kg/mm^2 on the Vickers scale), high modulus of elasticity (∼450-470 GPa) and low density (2.52 g/cm^3). The calculated covalent bond energy between boron and carbon is 9.42 eV, while the ionic bond energy is calculated to be 1.41 eV. These bond energies are consistent with the nature of the bonding being approximately 90% covalent. This high covalent property explains the extreme hardness and modulus of elasticity associated with boron carbide. Despite the high hardness of boron carbide, its high bonding strength, low coordination number (mainly due to covalent bonding), and lack of coated slip systems contribute to the resistance to dislocation motion, resulting in brittle mechanical behavior. Accordingly, the fracture hardness of boron carbide is usually low (2.9 - 3.7 MPa). Potential applications for sintered boron carbide materials are changing from machining and cutting and water jet cutting nozzles to high performance, lightweight armor. This property, along with its low fracture resistance and reactivity, makes boron carbide a useful material for nuclear reactor control rods or shielding plates (Wiley, 2011) (Schwetz, 2000). The (P/M) method consists of the steps of pressing metal powders inside a mold, bonding powder particles with each other, and sintering. This method is also a large process in which several materials are manufactured by pressing-sintering or hot pressing (Grum, 2006) (Schwetz, 2000). The primary element controlling the homogeneity of the reinforcement particle distribution in composites produced using the powder metallurgy approach is the matrix to reinforcement particle size ratio. The use of reinforcements with a larger average particle size will increase the homogeneity of the distribution. The mechanical characteristics also deteriorate when the reinforcing particle size grows as a result of slower work hardening and faster damage accumulation rates. In order to get the best performance, the microstructure must be optimized between smaller reinforcement particle size and more uniform spatial distribution (Slipenyuk et al., 2004). The aim of this study is to know the effect of rolling temperature and rolling ratio on the hardness and transverse rupture forces (TRS) on the composite (Cu-B_4C) and its effect on its microstructure and mechanical properties. 5 % wt. B_4C were added during the experiments to achieve this purpose. Manufactured by the (P/M) cold pressing method was used in all experiments. Scanning electron microscopy (SEM) and energy dispersive spectroscopy (EDS) were used to determine the microstructure and phase components of the sectors. Hardness tests were performed to measure its exact hardness and three-point bending tests were conducted to measure the bending strength.

2. Experimental procedures

In this Study, copper powder (Cu) with a purity of 99.9 % and a diameter of 40 µm , as well as boron carbide (B_4C) with a purity of 99.5 % and a diameter of 90 µm. To create the sample size (24mm x 10mm x 5mm) indicated in fig. 1, prepare the mold as illustrated in the drawing.

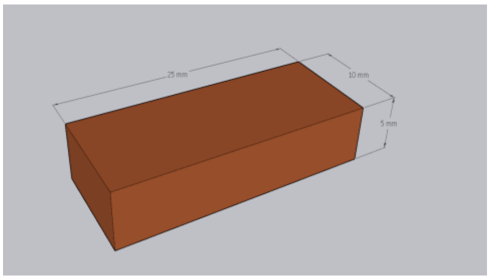

Figure 1: Sample

The copper (Cu) powders and the 5% wt. and boron carbide (B_4C) 95% wt. powders were combined for 60 min. at a speed of 45 r/min. To help with mixing, a total of 11 metal balls of various diameters were employed. A combination of powder to be pressed is placed into a mold during the pressing process, and the mold is then cold-pressed with 12.5 tons of pressure to create a sample of (24mm x 10mm x 5mm). The sintering temperature was 850°C, and the control system allowed the user to determine the process's duration and temperature. The temperature levels chosen in fig. 3 will be within 120 min. of the heating time, as illustrated in fig. 2. Both the hold and cooling times are 90 min. In this study, a maximum temperature of 850°C was used, with a heating rate of 25°C/min. The samples produced by compressing the powders under high pressure were sintered in a sintering furnace in a protected argon gas environment to boost their tensile strength.

Figure 2: Sintering Furnace

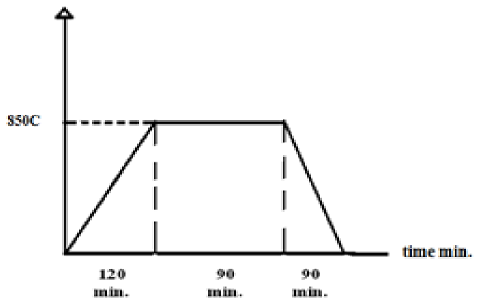

Figure 3: Cycle of temperature sintering

Hot-rolling was performed for samples that were sintered at 850°C for samples with a particle size of 90µm. When hot rolling at three different temperatures (600°C,700°C,800°C) with different reduction ratios (10%, 20%, 30%, 40%) in one direction, and to implement this, we used the rolling machine shown in fig. 4 It is located in the mechanical engineering laboratories of the University of Karabuk, where the speed of the rollers was 30 revs/min. and the diameter of the rollers was 70 mm, as shown.

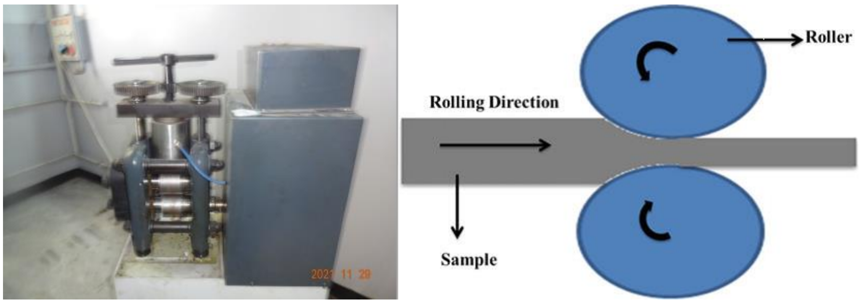

Figure 4: Rolling machine

Table 1: The final thickness of the samples after hot rolling Process

Rolling reduction ratio	Final thickness (tf)
% 0	5 mm
%10	4.5 mm
% 20	4 mm
% 30	3.5 mm
% 40	3 mm

3. Results and discussion

The microstructure and mechanical characteristics of items made by powder metallurgy are greatly influenced by density. Controlling the porosity in the microstructure allows one to alter the product's densification (Çelık & Aslan, 2017). Porosities' size, position, and shape are all crucial factors in the process of densification. Densification and the eradication of pores are determined by decreasing the surface area energy associated with pores. Greater values are found in the surface energy of pores than in the energy of grain borders (Çelık & Aslan, 2017). According to Table No. 1, the density values of the samples measured at room temperature by using Archimedes principle, and calculating the relative density to ascertain the porosity of the produced samples.

Table 2: Theoretical, Experimental density and Porosity values of the Control samples

Group No.	Grain size µm	Composites %wt.	Theoretical density g/cm^3	Experimental density g/cm^3	Relative density %	Porosity
1	90	Cu95%+B_4C5%	8.64	8.25	95.50	4.5

In order to determine the hardness of the samples obtained by hot pressing, the hardness of the samples was measured in Brinell via a Brinell hardness testing device with a load of 62.5 kg and a ball of 2.5mm diameter, as seen in fig. 5. In order to determine the hardness completely, hardness values were measured from the left and right surfaces of the samples, and a total of 5 hardness values were taken from each sample(Özkan ESKİa et al., 2017).

Figure 5: Brinell hardness measuring device

Table 3: The hardness values of the Rolled Samples at B4C grain size 90µm, 5% wt. B4C
Rolling temp. (600°C,700°C,800°C), Rolling rate (10%,20%,30%,40%)

Group No.	Grain sizes B4C µm	Composites %wt.	Sintering Temp.°C	Control Samples Hardness HB	Rolling ratio %	Rolling temp.°C 600°C	700°C	800°C
						Rolled samples Hardness		
1	90	Cu%95+B_4C%5	850°C	45	10	60	55	45
					20	61	56	44
					30	63	58	42
					40	65	60	40

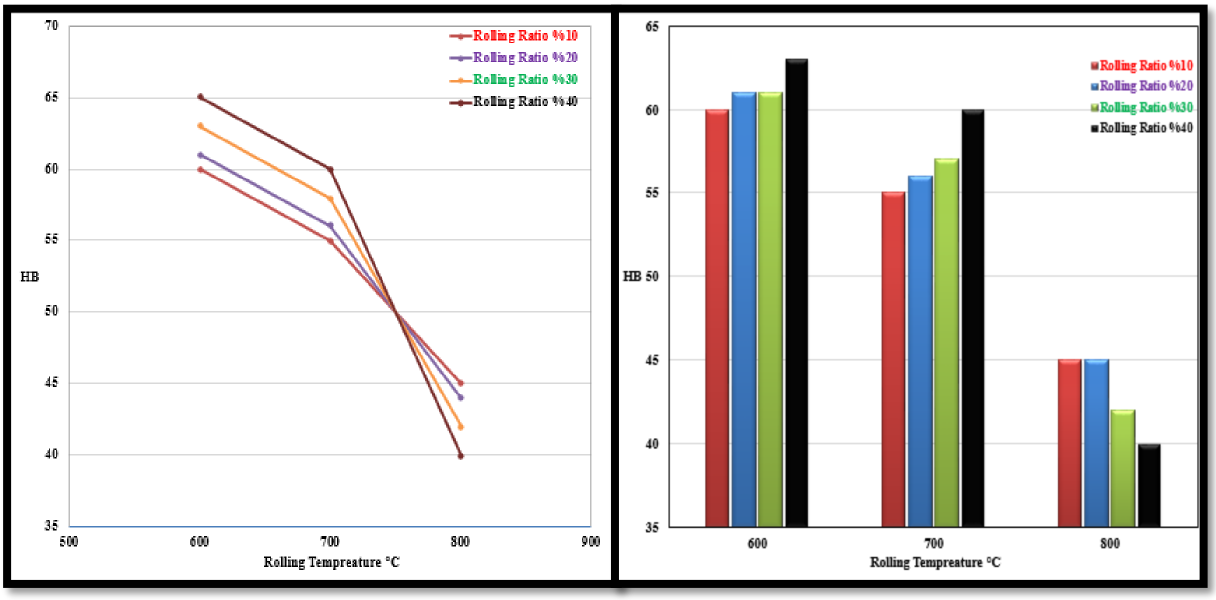

Figure 6: The relationship between hardness and the Rolling temp. (600°C,700°C,800°C), Rolled Samples At B4C grain size 90µm, 5 %wt. B4C, Rolling rate (10%,20%,30%,40%)

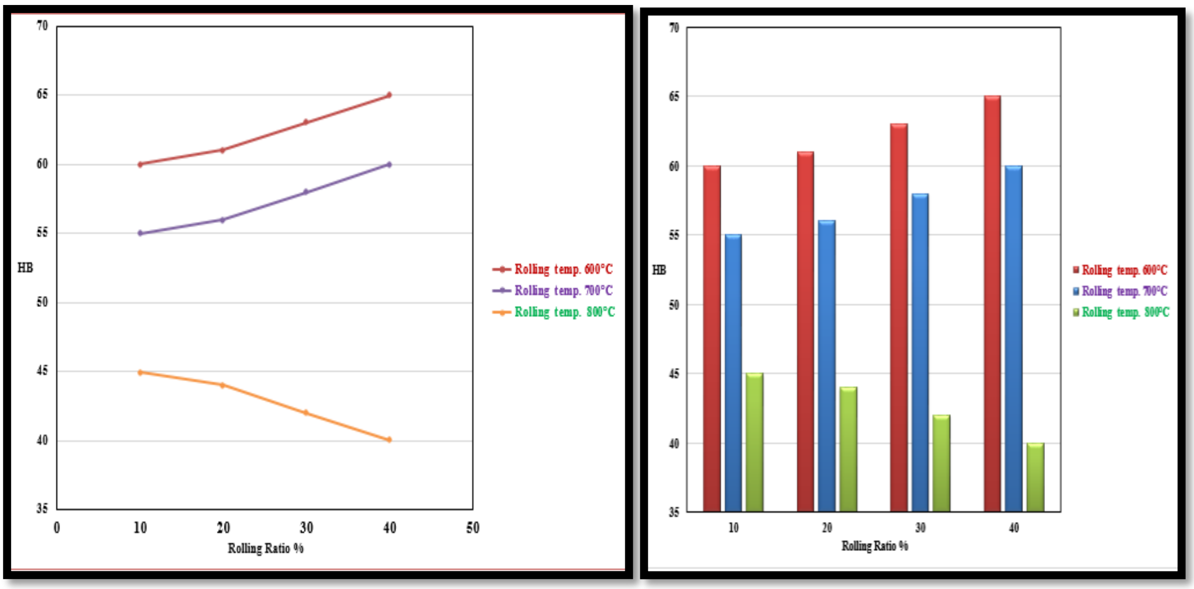

Figure 7: The relationship between hardness and the Rolling ration (10%,20%,30%,40%) Rolled Samples at B4C grain size 90µm, 5 %wt. B4C, Rolling temp. (600°C,700°C,800°C)

The hardness graphs of pure copper (Cu) subjected to the sintering process and the Cu-B_4C compounds produced with different rolling ratios (10%, 20%,30%,40%). When examining the results, the highest hardness values were obtaining from the compounds at a rolling temperature of 600°C and a rolling ratio of 40% is 65HBN, while the lowest hardness values obtain from the samples at a rolling temperature of 800°C and a rolling rate of 40% is 40HBN fig.8. Also note that at a rolling temperature of 600°C for all rolling ratios (10%,20%,30%,40%) the hardness is the highest. It decreased slightly at the rolling temperature of 700°Cfor all rolling ratios (10%, 20%,30%,40%) but notice a significant decrease at the rolling temperature of 800°C for all rolling ratios for all rolling ratios (10%,20%,30%,40%) (45 HBN,44 HBN,42 HBN,40HBN). However, the decrease in the hardness values at 800°C for all rolling ratios of (Cu-B_4C) can be attributed to the following reasons. A mismatch in the coefficient of thermal expansion between B_4C particles and the Cu matrix results in the generation of geometrically required dislocations around B_4C particles (Slipenyuk et al., 2004). With the decrease in B_4C content, the hardness decreased (Çelık & Aslan, 2017) . The hardness of the reinforcing element is higher than that of the matrix material, so the hardness of the composite material after the hot rolling process will be higher than that of the matrix material depending on the volume fraction before the rolling process. The reinforcement particles got closer to each other as the rolling temperature increased, which resulted in significant plastic deformation of the samples during the hot rolling process. These microstructural failures can be observed in lumpy regions of the matrix structure fig. 8 (a-b). As a result, micro voids, cracks, and failure patterns of the matrix material can result(Karakoç et al., 2018). After hot rolling with a rolling reduction ratio 40% deformation along its thickness. It can be seen fig.8(a-b) that high density dislocations and dynamic recrystallization exist in the (Cu-B_4C) matrix near the B_4C particles(Chen et al., 2018).

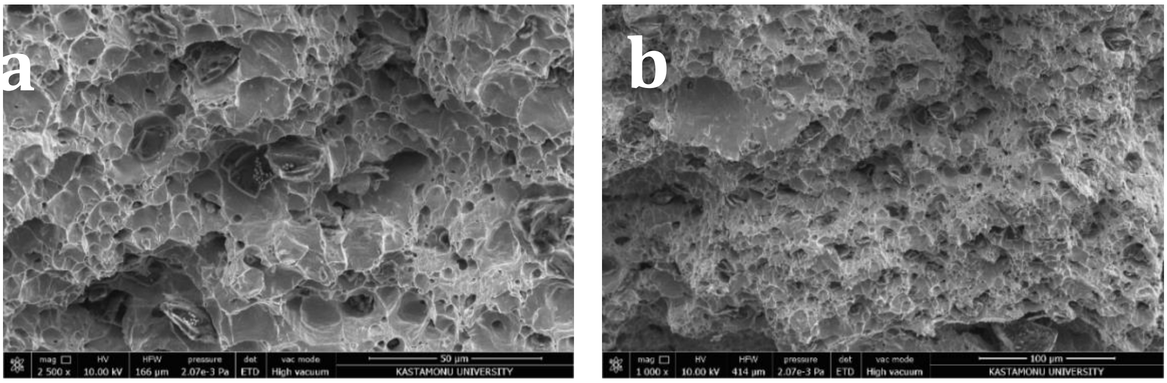

Figure 8: (a-b) SEM micrographs for sample B4C 5%wt. rolling ratio 20%, rolling temp.800°C different magnifications

4. The Transverse Rupture Forces (TRS) Test

To assess the bonding quality and determine the transverse rupture strength of the adherent copper matrix composites, three-point bending tests were performed using a SHİMADZU brand universal tensile machine with a maximum capacity of 50 k_N in Kastamonu University Laboratory at a testing speed of 0.5 $_{mm/min}$. fig.9. Samples with dimensions of (24_{mm} x10_{mm} x 5_{mm}) were used for the three-point bending test. It can be seen that the results of three-point bending experiments for 13 samples for each rolling temperature and rolling ratio.

Figure 9: Universal tensile test machine

Table 4: The Transverse Rupture Forces (TRS) values of the Rolled Samples at B4C grain size 90µm, 5% wt. B4C, rolling temp. (600°C,700°C, 800°C), Rolling rate (10%,20%,30%,40%)

Group No.	Grain sizes B_4C µm	Composites %wt.	Sintering Temp.°C	Control Samples TRS N/mm²	Rolling ratio %	Rolling temp.°C		
						600°C	700°C	800°C
						Rolled samples TRS N/mm²		
1	90	Cu%95+B_4C%5	850°C	483	10	472	440	437
					20	461	455	454
					30	455	526	526
					40	420	426	332

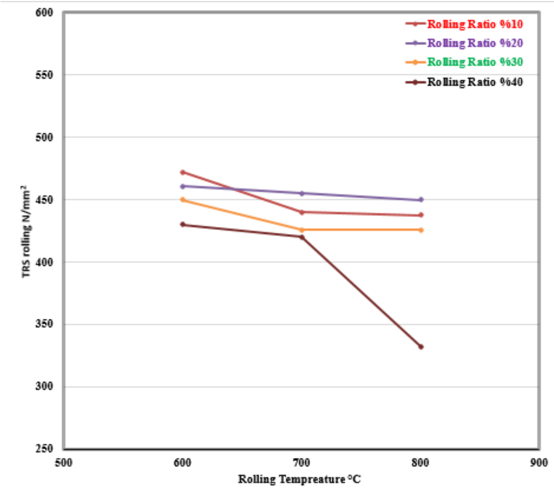

Figure 10: The relationship between The Transverse Rupture Forces (TRS) and Rolling Temperature (600°C,700°C,800°C) at B4C grain size 90µm, 5% wt. B4C, Rolling rate (10%,20%,30%,40%)

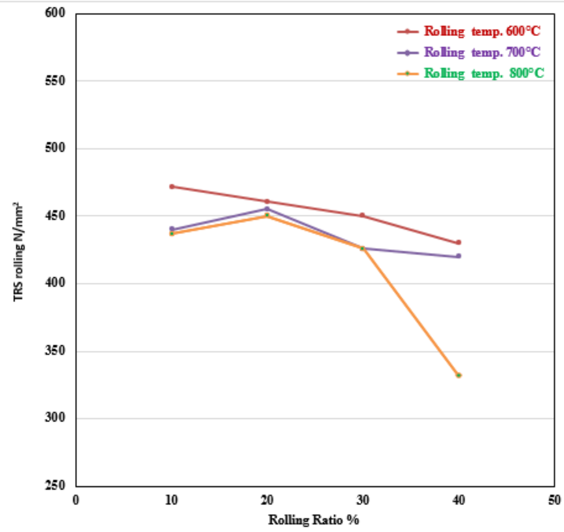

Figure 11: The relationship between The Transverse Rupture Forces (TRS) and the Rolling ration (10%,20%,30%,40%) Rolled Samples at B4C grain size 90µm, 5% wt. B4C, Rolling temp. (600°C,700°C, 800°C)

To determine the bonding quality of the copper matrix composites, three-point bending tests were performed using a 50 kN universal type tensile device according to ASTM B 528-83 with a test speed of 0.5 mm/min. Samples with dimensions of (24mm x10mm x5mm) were used for the three-point bending test of the original samples, that is, before the hot rolling process. As a result of the pressing process of the hot rolling process, the thickness of the samples decreased and became as follows: 10% of rolled samples have a thickness of (4.5mm) 20% have a thickness of (4mm) 30% have a thickness of (3.5mm) and 40% has a thickness of (3mm). The results of the three-point bending experiments for the 13 samples for each rolling temperature, rolling ratio, time, and pressure are summarized in Table 4.

Graphs of the transverse rupture forces (TRS) for pure copper under sintering and ($Cu-B_4C$) compounds produced with different rolling ratios Table 4, as shown in fig. (10-11). When examining the results, the highest values of (TRS) were obtained from the compounds for the original samples before the rolling process, at the sintering temperature of 850°C, hardness is 45HBN, TRS is 483 N/mm^2. The highest value (TRS) for the samples after the hot rolling process at the rolling temperature (700°C, 800°C) and the rolling pressure (30%, is 526 N/mm^2). The lowest values of (TRS) at a temperature of 800°C and the rolling pressure (40%, is 332 N/mm^2). In general, the value of (TRS) for all samples decreases as rolling ratios increase until reaching the lowest value at a 40% rolling ratio, is 332 N/mm^2 at rolling temperatures 800°C.

The reason for this is due to the occurrence of recrystallization and the mechanical properties of the materials were negatively affected by the heterogeneous distribution of the reinforcement particles in the matrix (Çelık & Aslan, 2017) (Balalan & Gulan, 2019).

5. Microstructure SEM-EDS

In this study, copper powder, 99.9% purity and 40μm diameter and boron carbide (B_4C) powder, 99.5% purity and 40μm diameter were used. SEM images of (Cu) powder and B_4C particles used in this study are shown in fig. 12 The (Cu) powder is spherical, and the B_4C particle is sharp-edged.

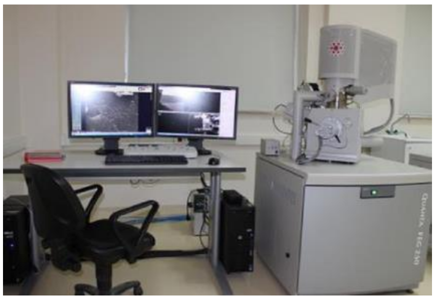

Figure 12: SEM device

The SEM micrographs for the different specimens sintered at 850°C are shown in fig. 13 (a-b) fig. 13 (a) controls the sample hardness value at 45 HBN, TRS at 483 N/mm^2, grain size 90 μm, and 5% wt. B_4C. fig. 13 (b) rolled sample hardness of 44 HBN, TRS of 454 N/mm^2, rolling ratio of 20% rolling temperature of 800°C, grain size of 90μm, and 5% wt. B_4C The magnification is 2500 times. The copper (Cu) side is seen as light-colored.

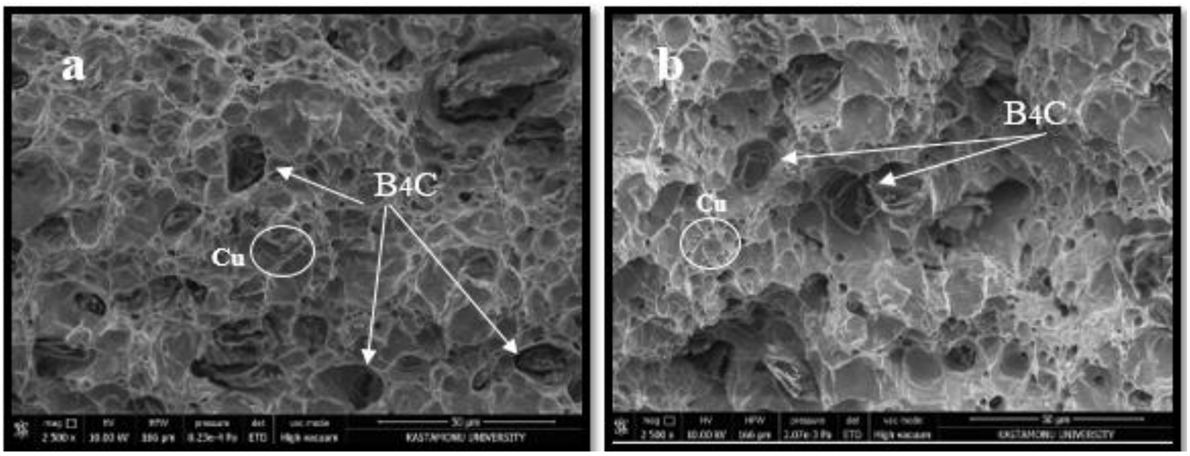

Figure 13: SEM images of the specimen sintering temp.850°C, 5% wt. B4C, (a). Control sample (b) Rolled sample at rolling temp.800°C, rolling ratio 20%

regions, while the black angle shapes indicated boron carbide (B_4C) particles. The (B_4C) is observed to be uniformly distributed on the compost side of the copper matrix composite, and some pores were observed in the compounds (ESKi&ELHEMSHERI, 2021)

Scanning electron microscope (SEM) examinations were conducted on pure Cu powder and on composites reinforced with different 5% wt. B_4C. They are presented in fig. 13 (a–b) at various (×2500) magnifications. It can easily be seen that the B_4C particles are distributed homogenously in the matrix and no segregation takes place at a particular region. However, presences of the porosity of the B_4C particles are observed(Topcu et al., 2009). Composites The fracture surfaces of homogeneous Cu -B_4C and Cu -B_4Composites were signed and shown in fig. 13 (b). It could be seen that the dimples in the 5% wt. Cu -B_4C composites were most obvious and deepest because of the effect of maximum cu content among these composites. In other words, the higher the content of (cu), the fracture form of composites tends to be that of metals when ductile. (Zhang et al., 2020) explains that this decrease is connected to the density of the pores and lubricants, which results in a decrease in composite material density with increased reinforcing rate (Okay & Islak, 2022).

The SEM images taken from the fracture surfaces of the samples subjected to the three-point bending test are examined fig. 13 (a-b). The small grain size causes B_4C to be positioned in the gaps in the matrix, and thus the reinforcing element is homogeneously distributed in the matrix. The fracture form in the sample is brittle. Brittle fracture occurs by creating a notch effect in boron carbide grains. The quantitative variation of (Cu), (B), and (C) elements is observed from B_4C particles to the Cu matrix through the interface. It is observed that as we move from B_4C particles to a (Cu) matrix, the quantitative value of (B) gradually decreases and (Cu) increases.

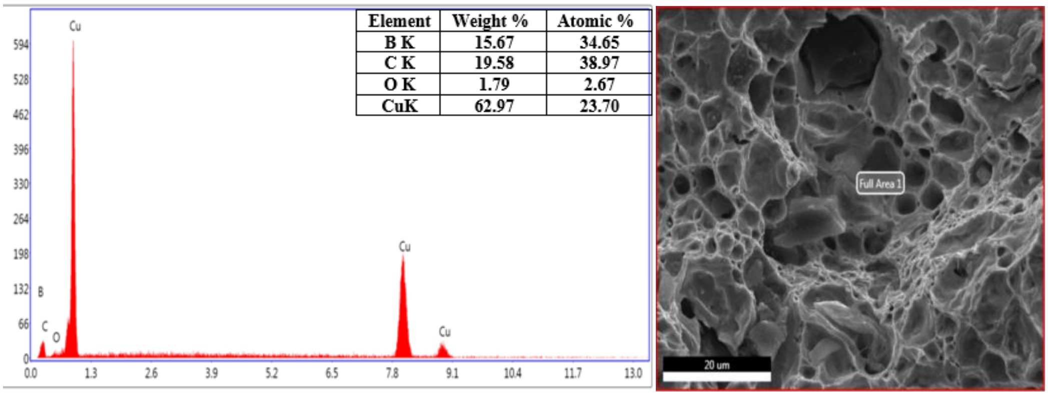

Figure 14: SEM -EDS data of Copper composite matrix sample containing 5% wt. B4C, Control sample

Fig. 14 shows the presence of boron (16.74% wt.) carbon (15.75% wt.), copper (65.07) and oxygen (2.44) elements in the structure of SEM and EDS analysis. This proves the presence of boron carbide in the composite structure. In the SEM image, dark areas indicate B_4C, and the remaining gray areas indicate (Cu) matrix. Upon examination of the other samples it is seen that (B_4C) and (C) peaks form and there are increases in the intensities of these peaks with increasing reinforcement rate. No new phase forms in the structure. It is also understood from EDS analysis that oxide forms even partially depending on the increasing temperature on the surface. There were small amounts of oxygen elements in copper and composite samples fig. 14 This probably resulted from the oxidation of the matrix during sintering.(Altinsoy et al., 2013) The small amount of oxygen that EDX found is thought to have resulted from an oxide layer that formed during specimen preparation.(Shorowordi et al., 2003)

Fig. 15 shows the presence of boron (16.67% wt.) carbon (19.85% wt.), copper (62.97% wt.) and oxygen (1.79) elements in the structure of SEM and EDS analysis. This proves the presence of boron carbide in the composite structure. In the SEM image, dark areas indicate B_4C, and the remaining gray areas indicate (Cu) matrix. There were small amounts of oxygen elements in copper and composite samples fig. 15. This probably resulted from the oxidation of the matrix during sintering.(Altinsoy et al., 2013) There is a good bonding between copper matrix and B_4C particles. Probably for this reason oxygen contents in the surface maps decreased with increasing particle size of B_4C(Celebi Efe et al., 2012).

The fracture surfaces shown in fig. 16 (a-b) of both the hot-rolled composite samples were analyzed by SEM - EDS micrographs. From SEM - EDS analyses, we observed that B_4C molecules are included in the matrix structure graphs. From SEM - EDS analyses, we observed that B_4C molecules are included in the matrix structure. Cross-granular cracks occurred on the B_4C particles without separating from the matrix. The B_4C particles remaining in the fractured surface after the bending test are evidence of good interconnection between the matrix and the reinforcement particles. Thus, it can be assumed that the other side of the cracked B_4C particles retained the other part of the fractured surface. The embedded B_4C particles act as a crack sealer and prevent rapid crack progression through the matrix structure. Thus, the deformation of the compounds was limited, which improved the TRS of the samples. However, some cracking effects were observed on the fracture

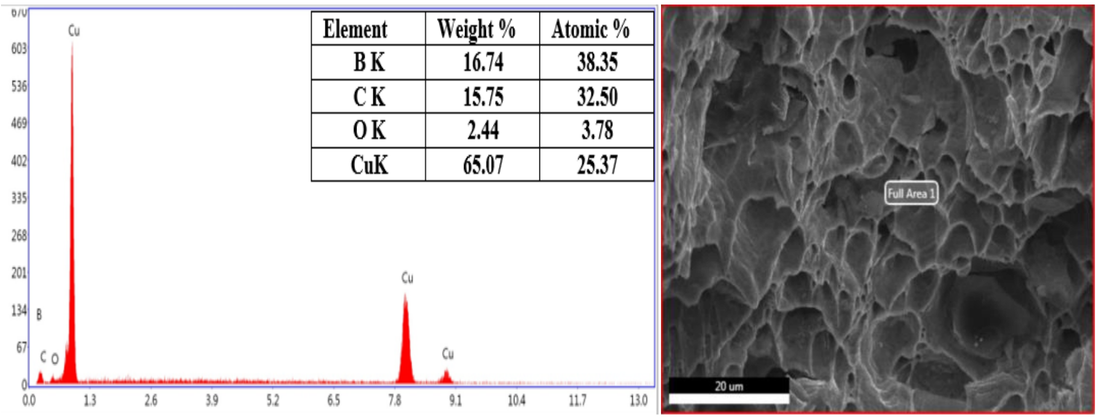

Element	Weight %	Atomic %
B K	16.74	38.35
C K	15.75	32.50
O K	2.44	3.78
CuK	65.07	25.37

Figure 15: SEM - EDS data of Copper composite matrix sample containing 5% wt. B4C, rolled sample at rolling temp.800°C, rolling ratio 20%

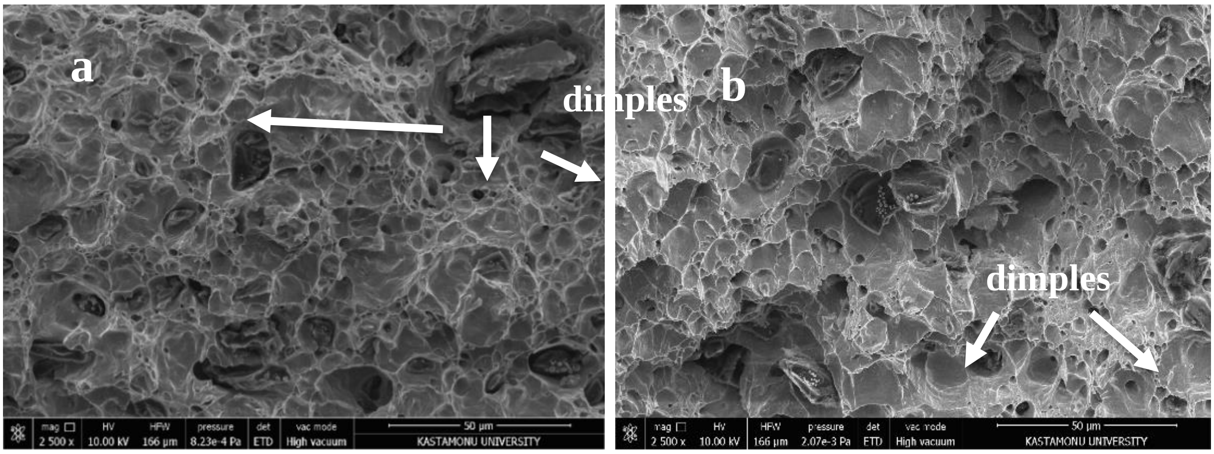

Figure 16: SEM images of the specimen sintering temp.850°C, 5% wt. B4C, (a). Control sample (b) Rolled sample at rolling temp.800°C, rolling ratio 20%

surfaces of the hot-rolled samples due to the applied rolling pressure causing the forced movement of the dislocation. The presence of large, deep voids and small dimple shapes on the fractured surface shows good ductility for both composite and hot-rolled samples(Karakoç et al., 2018). Fracture surfaces shown in fig. 16 (a-b) reveal the dimples in the structure, which is an indication of ductile fracture. Ductile fracture takes place by the nucleation, growth, and coalescence of microvoids, which lead to a crack (Ramesh et al., 2018). Fig. 16 (a-b) shows fracture surfaces specimens. Practically no difference in dimple size is observed between the specimen control sample fig. 16 (a) and after hot rolling fig. 16 (b) rolling Process. Other than dimpled surface, the specimens show flat surface of area fraction as a result of grain boundary fracture(Chen et al., 2018).

6. Conclusion

- SEM-EDS studies reveal that it is clear that B_4C particles are homogeneously distributed and dominantly occupy around copper grains.
- EDS analyses of composites show that the main components of (Cu–B_4C) composites are copper and B_4C, and a small amount of oxide was found on the free surface of B_4C particles, especially for composites rolled at 800°C.
- The hardness of composites (Cu-B_4C) is increased as the rolling ratio is increased at the same rolling temperature.
- The maximum hardness of the samples is measured at a rolling rate of 40% and a rolling temperature of 600°C is 65 HBN. At a rolling ratio of 40% at 800°C, the hardness value is the lowest at 40 HBN. It is important to note that the highest hardness values for all samples are at a rolling temperature of 600°C for all different rolling ratios (10%,20%,30%,40%). It is worth noting that the lowest hardness values

were obtained for all samples at a rolling temperature of 800°C and for all different rolling ratios (10%,20%,30%,40%).

- It is considered that the most important reason for the breakup of B_4C reinforcing material is that composite (Cu-B_4C) specimens relatively had a porous structure, and these particles having a hard construct caused cavities on the surface of specimens.
- Added B_4C reinforcements help in strengthening of the composite by inducing dislocation strengthening mechanisms by obstructing dislocation mobilities at interfaces.
- As the rolling ratio and rolling temperature are increased, the hardness decreases until it reaches the lowest value of 40 HBN at a rolling ratio of 40% and a rolling temperature of 800°C when the sample thickness is 3mm.As the rolling ratio and rolling temperature are increased, the (TRS) decreases until it reaches the lowest value of 332 N/mm^2 at a rolling ratio of 40% and a rolling temperature of 800°C when the sample thickness is 3mm.

Contribution statement for authorship

Özkan ESKi: Investigation, Supervision, Software, Validation.
Hasan ALSead Ibrahim ENBIA:
Conceptualization, Methodology, Software, Data Curation,

Declaration of Competing Interest

The authors declare that they have no known competing financial interests or personal relationships that could have appeared to influence the work reported in this paper.

Acknowledgments

We would like to express our sincere gratitude and appreciation to all the employees of the central laboratories of Kastamonu University and the University of Karabuk Mechanical Engineering Laboratories for their cooperation and support throughout the duration of this work.

References

Altinsoy, I., Celebi Efe, F. G., Aytaş, D., Kılıç, M., Ozbek, İ., & Bindal, C. (2013). Some Properties of Cu-B4C Composites Manufactured by Powder Metallurgy. Periodicals of Engineering and Natural Sciences (PEN), 1(1), 34–38. https://doi.org/10.21533/pen.v1i1.14

Balalan, Z., & Gulan, F. (2019). Microstructure and mechanical properties of Cu-B4C and CuAl-B4C composites produced by hot pressing. Rare Metals, 38(12), 1169–1177. https://doi.org/10.1007/s12598-019-01287-2

Celebi Efe, G., Altinsoy, I., Ipek, M., Zeytin, S., & Bindal, C. (2012). Effects of SiC particle size on properties of Cu-SiC metal matrix composites. Acta Physica Polonica A, 121(1), 251–253. https://doi.org/10.12693/APhysPolA.121.251

Çelık, E., & Aslan, A. K. (2017). The effect of porosity and cu rate on microstructure and mechanical properties of co alternative powder metallurgy compound. Science of Sintering, 49(3), 225–234. https://doi.org/10.2298/SOS1703225C

Chandra, B., Kumar, J., Singh, H., & Kumar, J. (2015). Production technologies of metal matrix composite-A Review. 4th International Conference on Advances in Materials and Manufacturing Technology (AMMT-14), 5762(June 2015), 9.

Chen, H. S., Wang, W. X., Nie, H. H., Zhou, J., Li, Y. L., Liu, R. F., Zhang, Y. Y., & Zhang, P. (2018). Microstructure evolution and mechanical properties of B4C/6061Al neutron absorber composite sheets fabricated by powder metallurgy. Journal of Alloys and Compounds, 730, 342–351. https://doi.org/10.1016/j.jallcom.2017.09.312

ESKi, Ö., & ELHEMSHERI, M. A. M. (2021). Effect of bonding time and boron carbide percentage on diffusion bonding characteristics for copper/copper matrix composites (Cu + Cu%B4C). Materials Today: Proceedings, xxxx. https://doi.org/10.1016/j.matpr.2021.05.342

Grum, J. (2006). Book Review: Powder Metallurgy and Particulate Materials Processing: The Processes, Materials, Products, Properties, and Applications. International Journal of Materials and Product Technology, 27(3/4), 290. https://doi.org/10.1504/ijmpt.2006.011278

Karakoç, H., Karabulut, Ş., & Çıtak, R. (2018). Study on mechanical and ballistic performances of boron carbide reinforced Al 6061 aluminum alloy produced by powder metallurgy. Composites Part B: Engineering, 148(April), 68–80. https://doi.org/10.1016/j.compositesb.2018.04.043

Konen, R., & Fintov, S. (2012). Copper and Copper Alloys: Casting, Classification and Characteristic Microstructures. Copper Alloys - Early Applications and Current Performance - Enhancing Processes, 3–31. https://doi.org/10.5772/39014

Okay, F., & Islak, S. (2022). Microstructure and Mechanical Properties of Aluminium Matrix Boron Carbide and Carbon Nanofiber Reinforced Hybrid Composites. Science of Sintering, 54(2), 125–138. https://doi.org/10.2298/SOS2202125O

Özkan ESKİa, ISLAKb, S., & URAYLI, Ç. (2017). The Effect of Boron Carbide Amount on Microstructure and Electrical Properties of Cu-B 4 C Composite Materials. 1st International Conference of Advanced Materials and Manufacturing Technologies (ICAMT), 1(October), 25–27.

Ramesh, S., Nayaka, H. S., Anne, G., & Gopi, K. R. (2018). Influence of cold rolling process on microstructure and mechanical properties of Cu-1.5%Ti alloy. AIP Conference Proceedings, 1943. https://doi.org/10.1063/1.5029631

Sahu, P. S., & Banchhor, R. (2016). Fabrication methods used to prepare Al metal matrix composites- A review. International Research Journal of Engineering and Technology, 03(10), 123–132.

Saravanapandi Solairajan.Aa*, A. S., Balavignesh.Pc, P. S., a*, b Assistant Professor, D. of M. E., Infant Jesus college of Engg & Tech, Keelavallanadu, Tuticorin, I., c, d UG Student, D. of M. E., Infant Jesus college of Engg & Tech, Keelavallanadu, Tuticorin, I., & A*solairajan2k@gmail.com. (2007). PROCESSING TECHNIQUES AND APPLICATIONS OF METAL MATRIX COMPOSITES. 5.

Schwetz, K. A. (2000). Boron Carbide, Boron Nitride, and Metal Borides. Ullmann’s Encyclopedia of Industrial Chemistry. https://doi.org/10.1002/14356007.a04_295

Shorowordi, K. M., Laoui, T., Haseeb, A. S. M. A., Celis, J. P., & Froyen, L. (2003). Microstructure and interface characteristics of B4C, SiC and Al2O3 reinforced Al matrix composites: A comparative study. Journal of Materials Processing Technology, 142(3), 738–743. https://doi.org/10.1016/S0924-0136(03)00815-X

Slipenyuk, A., Kuprin, V., Milman, Y., Spowart, J. E., & Miracle, D. B. (2004). The effect of matrix to reinforcement particle size ratio (PSR) on the microstructure and mechanical properties of a P/M processed AlCuMn/SiCp MMC. Materials Science and Engineering A, 381(1–2), 165–170. https://doi.org/10.1016/j.msea.2004.04.040

Topcu, I., Gulsoy, H. O., Kadioglu, N., & Gulluoglu, A. N. (2009). Processing and mechanical properties of B4C reinforced Al matrix composites. Journal of Alloys and Compounds, 482(1–2), 516–521. https://doi.org/10.1016/j.jallcom.2009.04.065

Wiley, C. S. (2011). HIGH-STRENGTH AND LOW-COST BORON CARBIDE HIGH-STRENGTH AND LOW-COST BORON CARBIDE. May.

Zhang, L., Shi, G., Xu, K., Hao, W., Li, Q., Junyan, W., & Wang, Z. (2020). Phase transformation and mechanical properties of B4C/Al composites. Journal of Materials Research and Technology, 9(2), 2116–2126. https://doi.org/10.1016/j.jmrt.2019.12.042